

Influence of the Precipitation Agent in the Deposition–Precipitation on the Formation and Properties of Au Nanoparticles Supported on Al₂O₃

J. Radnik,* L. Wilde, M. Schneider, M.-M. Pohl, and D. Herein

Leibniz-Institute for Catalysis at the University of Rostock (former ACA), Richard-Willstätter-Str. 12, 12489 Berlin, Germany

Received: August 25, 2006; In Final Form: September 14, 2006

Au nanoparticles supported on Al₂O₃ were prepared by deposition–precipitation of HAuCl₄ with different precipitation agents NaOH and urea. The samples were investigated by means of different characterization techniques such as X-ray photoelectron spectroscopy (XPS), X-ray absorption spectroscopy (XAS), and transmission electron microscopy (TEM). The results show that depending on the precipitation agent, the Au particles have a different Au–Au coordination number and size after calcination at 523 K. Whereas the use of NaOH leads to the formation of Au nanoparticles with a Au–Au coordination number of 6.7 and a mean diameter below 2 nm, those prepared with urea have a mean size of 3.1 nm. The Au–Au coordination number could be determined as 8.6. At the smaller particles obtained with NaOH, hints for Au–O interactions were found. For these particles TEM results advise a rather flat lenticular morphology. Different deposition mechanisms depending on the precipitation agent are discussed as the reason for the formation of nanoparticles with different shapes, sizes, and valence states.

Introduction

Since the discovery of their high catalytic activity for the low-temperature CO-oxidation,¹ gold catalysts have attracted much attention. It has been shown that gold becomes active for many reactions when stabilized in the form of nanoparticles attached to metal oxide and carbon supports.^{2–4} One problem that complicates the commercialization of gold catalysts is the preparation, which is often not reproducible and requires precise control of the preparation conditions. Two preparation techniques have good potential for commercialization: (i) the coprecipitation method using mixed precursors of Au and the metal component of the support and (ii) deposition–precipitation. Here, the pH of an aqueous solution of HAuCl₄ is adjusted at a fixed value between 6 and 10. The control of the pH and of the temperature allows the selective deposition of Au(OH)₃ only on the surfaces of the support without precipitation of gold in the liquid phase. NaOH⁵ or urea⁶ are mostly used as precipitation agents. The advantage of urea is that all the gold in the solution is deposited on the support, as shown in the case of TiO₂. Due to this reason, a higher gold loading can be achieved and the deposition is better reproducible. Recently, Zanella et al. investigated with different characterization techniques such as X-ray absorption spectroscopy (XAS), transmission electron microscopy (TEM), and catalytic testing in the CO oxidation⁷ in which way different precipitation agents such as NaOH and urea influence the formation and properties of gold nanoparticles supported on TiO₂. They found that the temperature needed for the reduction of Au(III) to Au(0) depends on the precipitation agent. The reduction starts at 373 K for the catalyst prepared with NaOH and at 423 K for the sample using urea as precipitation reagent. This result was explained with a different deposition mechanism of gold on the support. After calcination at 473 K no differences in particle size, oxidation state and chemical reactivity were obvious.

In a recently published work nanoscale gold catalysts on Al₂O₃ support were developed for the partial oxidation of

polyvalent oxygen-substituted compounds such as ethylene glycol, glyoxal, and selected saccharides.⁸ In contrast to results obtained for Au nanoparticles on TiO₂, an influence of precipitation agent on the chemical reactivity of these Al₂O₃-supported gold catalysts calcined at 523 K could be observed. The catalysts prepared with NaOH were more active in the oxidation of ethylene glycol to glycolic acid than the samples analogically prepared with urea, whereas both catalysts contained around 2.7 wt % Au. Differences in the chemical activity of the gold nanoparticles supported by Al₂O₃ were confirmed by O₂-chemisorption measurements. These chemical results were explained by different particle sizes, whereas larger gold particles seem to be found at the catalyst prepared with urea.

It is well-known that the particle size is correlated with the Au–Au coordination number; i.e., in smaller particles the Au–Au coordination number is lower than that in larger ones. Next to the size the particle shape influences the Au–Au coordination number. It was recently shown for the CO oxidation that this coordination number is dominant and crucial for the catalysis by Au.⁹ Additionally, an influence of the electronic structure of the gold particles on the chemical activity is discussed in the literature.^{10–14}

Detailed investigations of the Al₂O₃-supported Au catalysts with spectroscopy and microscopy (TEM, XAS, XPS) were made to elucidate the geometric structure and the electronic states of the gold particles dependent on the used precipitation agent NaOH or urea. From these investigations an explanation of the different chemical activity of the Al₂O₃-supported gold particles prepared either with urea or with NaOH could be expected. Further insights of the influence of the precipitation agent on the deposition of gold nanoparticles on oxidic nanoparticles should be gained.

Experimental Section

The catalysts were prepared by deposition–precipitation using HAuCl₄ and γ -Al₂O₃ (Puralox HP14/150, S_{BET} = 151 m²/g).

Although the preparation methods are reported elsewhere in detail,¹⁵ for a better understanding of this article several steps of the preparation are summarized again.

Preparation. Au/Al₂O₃ (NaOH). Alumina powder was suspended in deionized water. The pH of the suspension was pre-adjusted to 7 at 343 K by diluted NaOH. An aqueous solution of HAuCl₄·3H₂O was subsequently added drop-by-drop into the neutralized suspension, along with a 0.1 N NaOH solution to maintain the pre-adjusted pH. After the resulting solution was stirred for 1 h at 343 K and cooled to room temperature, a Mg citrate solution preadjusted to pH 7 with diluted NaOH was added to the slurry and the suspension was further stirred for 1 h. The solid was separated from the liquid by centrifugation, washed with distilled water free from chloride, and dried under vacuum at a pressure <50 kPa at room temperature and at 323 K. Finally, the sample was calcined at 523 K for 3 h (heating rate = 1 K/min). To check the influence of the pH on the preparation, samples were made with solutions pre-adjusted at pH values of 8 and 9.

Au/Al₂O₃ (Urea). An aqueous solution of HAuCl₄·3H₂O containing chloroauric acid and an excess of urea was added to Al₂O₃ suspended in deionized water. The mixture was stirred, heated to 343 K, and kept at this temperature to ensure a slow and gradual increase of the pH value by hydrolysis of urea. After reaching pH 6.8, which is the maximum pH value that could be obtained with this method, the suspension was cooled to room temperature. A Mg citrate solution pre-adjusted to a pH of 7 was added and the suspension was stirred for 1 h. Subsequently, the preparation was continued as described above.

The Au amount of the samples was determined by the inductively coupled plasma emission spectrometer (ICP-OES) iOptima 300XL (Perkin-Elmer) after chemical pulping with nitrohydrochloric and hydrofluoric acids.

The samples prepared at pH 7 using the two different precipitation agents with a similar Au content of 2.78 wt % (Au/Al₂O₃ (NaOH)) or 2.60 wt % (Au/Al₂O₃ (urea)) were characterized by the following techniques to investigate the influence of the precipitation agent on the Au particles.

TEM. For TEM investigations a Philips CM20 ST, equipped with EDXS (EDAX, PV9900), was used at 200 kV. The samples were prepared by depositing the catalysts directly on copper grids with Lacey-Carbon.

XPS. The photoelectron spectroscopy measurements were carried out at VG ESCALAB 220iXL with Mg K α radiation ($E = 1253.6$ eV). The samples were fixed by a double-sided adhesive carbon tape on the stainless steel sample holder. The electron binding energy was referenced to the Al 2p peak of Al₂O₃ at 74.4 eV. The peaks were fitted by Gaussian–Lorentzian curves after a Shirley background subtraction. For quantitative analysis the peak area was divided by the element-specific Scofield factor and the transmission function of the analyzer. The background pressure in the chamber was better than 10^{−7} Pa.

XAS. XAS measurements (fluorescence mode) at the Au L_{III} edge ($E = 11.919$ keV) were taken at the beamline A1 of HASYLAB (Hamburg, Germany). The samples were mixed with boron nitride and pressed to pellets with a force of 1 ton maximum, to avoid pressure-induced structural changes of the nanoparticles. As standard sample, a 5 μ m thick Au foil (99.999%) was measured in transmission mode. Data acquisition time for each spectrum in fluorescence mode was about 30 min. To improve the signal/noise ratio, two or three spectra of one sample were added up. The data were analyzed using WinXAS 2.1 to normalize the raw spectra for the absorption edge step

TABLE 1: Comparison between the Offered Au Content and the Precipitated Au Loading Determined by ICP-OES

precipitation agent	pH	offered Au [%]	precipitated Au [%]	ratio prec./off.
urea	7	3.00	2.60	0.9
NaOH	7	1.50	0.95	0.6
	8	1.50	0.40	0.3
	9	1.50	0.15	0.1
	7	4.00	2.78	0.7

height and to extract the EXAFS function by the subtraction of the atomic background function and subsequent Fourier transformation.¹⁶ Further data analysis was performed using the MS code FEFF 7 to calculate the theoretical scattering parameters.¹⁷

Results

To obtain a geometric model for the Au particles, TEM and EXAFS measurements were made. TEM does make some statements on the size and morphology of the Au particles; the local surroundings of the Au could be derived from EXAFS. Information about the electronic structure was gained by XANES and XPS investigations. An influence of the precipitation agent on the properties of the particles could be observed with all methods.

Influence of the pH and the Precipitation Agent on the Au Loading. As described above, Au was deposited on Al₂O₃ at different pH values between 7 and 9 with NaOH as precipitation agent. Such procedures were not possible for urea because it was impossible to obtain higher pH values than 7 with this method. In Table 1 the results for the deposited Au content determined with ICP-OES are presented and compared with the offered Au amount in the solution. The ratio between deposited and offered Au decreases with increasing pH in the range between pH 7 and 9. Similar to the published results with TiO₂ as support, the preparation with urea was more efficient for depositing Au on the oxidic support. To obtain further insights into the influence of the precipitation agents, the samples with a comparable Au content of ca. 2.7 wt % prepared at the same pH were chosen for the detailed characterization.

TEM. Some information about the size and morphology of the particles could be obtained by TEM investigations. Both samples show small particles (Figure 1), but they differ both in average diameter and particle size distribution (Figure 2). In

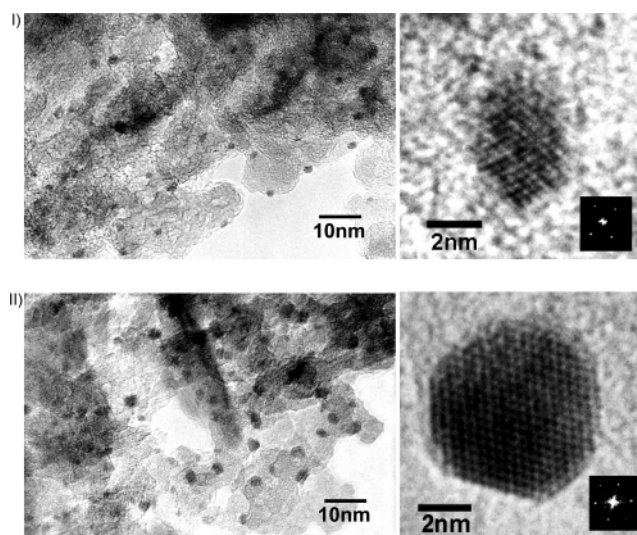


Figure 1. TEM images of (I) Au/Al₂O₃ (NaOH) and (II) Au/Al₂O₃ (urea). Both samples were calcined at 523 K.

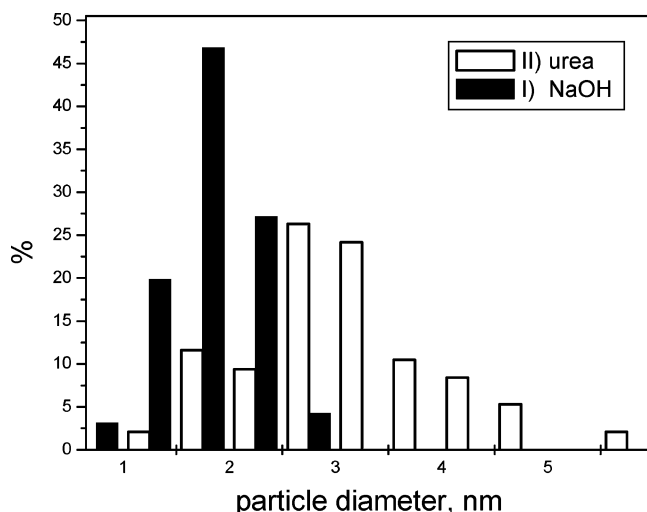


Figure 2. Size histograms of both Au/Al₂O₃ samples determined by TEM.

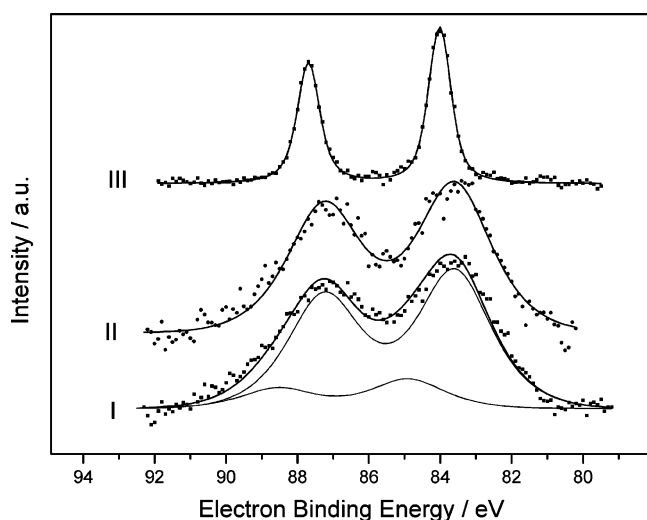


Figure 3. Background subtracted and normalized XP spectra (Au 4f) of the supported Au nanoparticles (I: Au/Al₂O₃ (NaOH); II: Au/Al₂O₃ (urea)), and as reference of Au foil (III). The fit parameters are summarized in Table 2. The samples with Al₂O₃ as support were calcined at 523 K.

Au/Al₂O₃ (NaOH) most Au particles have a size in a range from 1 to 3 nm with an average particle size of 1.9 nm (calculated from 96 particles). Beside these small particles a few particles with diameters of about 10 nm were detected (not shown in Figure 1). Due to the difficulties in evaluating their amount, the average size was calculated only for the smaller ones. In Au/Al₂O₃ (urea) a much broader distribution of the Au particle size is observed (Figure 2), with particle sizes between 1 and 6 nm and an average size of 3.1 nm (calculated from 95 particles). In contrast to Au/Al₂O₃ (NaOH), this sample showed no indication for particles larger than 10 nm.

The high-resolution images show in both cases crystalline gold particles. The inserted power spectra are indexed as a [100] zone axis for the more elongated particle in the case of NaOH and a [101] zone axis for the spherical particle in the second case (urea). This difference in shape was found only for a few particles in the NaOH case.

XPS. To obtain further information about the electronic states of the samples, X-ray photoelectron measurements were carried out. In Figure 3 the background-corrected spectra for both samples and of a gold foil as a reference are presented, whereas in Table 2 the fit results for both samples are compared with

TABLE 2: Results of the Fitting of the Au/Al₂O₃ Samples Compared with Bulk Au

sample	binding energy [eV]	doublet splitting [eV]	fwhm [eV]	ratio of Au states	c(Au)/c(Al) determined by XPS
urea	83.8 (±0.2)	3.7	2.5		0.003
NaOH	(i) 83.8 (±0.2)	3.7	2.5	(84 ± 4) %	0.006
	(ii) 85.1 (±0.2)	3.7	2.5	(16 ± 4) %	
Au foil	84.0 (±0.2)	3.7	1.1		

the results obtained for gold foil under the same measurement conditions. For Au/Al₂O₃ (NaOH) two states could be detected: a more intense state with an electron binding energy of 83.8 eV and a less abundant one at 85.1 eV. Only the state with the lower binding energy was observed for the sample prepared with urea. This electron binding energy could be correlated with metallic Au. The higher electron binding energy of 85.1 eV is typical for partially oxidic Au, but it is too low for known pure stable Au oxides. The width of both peaks is in the case of the supported Au particles, clearly broader than that for the metal foil used as reference data, but this is a well-known phenomenon for small particles.¹⁸ The observation of TEM indicating smaller particles in the case of Au/Al₂O₃ (NaOH) is confirmed by comparing the Au/Al ratio of both samples obtained by quantitative analysis, which is a measure for Au dispersion. This ratio is for Au/Al₂O₃ prepared with NaOH (0.006), twice as high as observed for the sample with urea as the precipitation agent (0.003).

XAS. XANES. Next to XPS, the electronic states of the Al₂O₃-supported gold nanoparticles were investigated with XANES. As references, the spectra of Au(III) (HAuCl₄) and Au(0) (Au foil) were recorded. In Figure 4 the normalized XANES spectra of these four samples are presented. A comparison with literature data shows a strong similarity between the spectrum of HAuCl₄ presented here and those of Au(OH)₃ or Au₂O₃,^{7,19} which can be explained by the hydrolysis of a major part of the HAuCl₄ to Au(OH)₃. The absorption edges of the samples with the supported gold nanoparticles are more or less at the same value as the edge of the Au foil, indicating that gold is zerovalent. For a more detailed analysis, the near-absorption edge region was scanned with a step width of 0.25 eV and difference spectra between the spectra of the supported gold particles and the spectrum of the Au foil were calculated (I–III; II–III). For Au/Al₂O₃ (NaOH) a small positive peak around 11.92 eV was

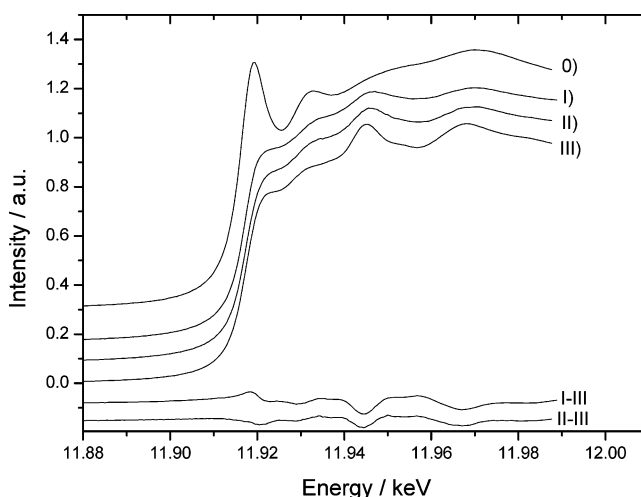


Figure 4. Normalized XANES spectra (Au L_{III} edge) of references (0: hydrolyzed HAuCl₄, III: Au(foil)) and the supported Au nanoparticles (I: Au/Al₂O₃ (NaOH); II: Au/Al₂O₃ (urea)). The samples with Al₂O₃ as support were calcined at 523 K. Difference spectra are labeled.

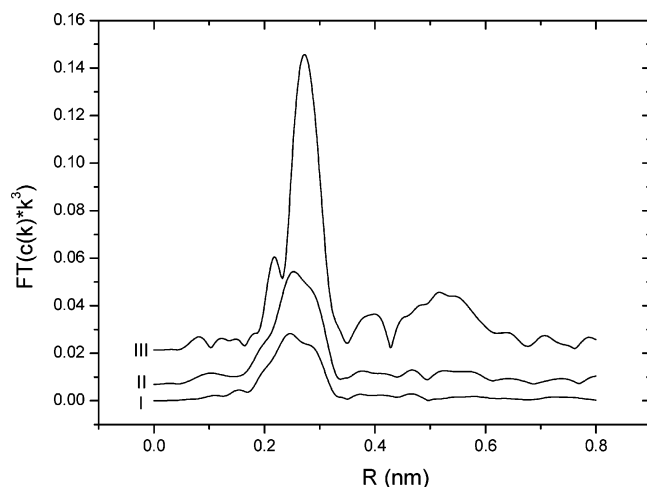


Figure 5. Modulus of the Fourier transform of the EXAFS signals of Au(foil) as reference (III) and both samples I: Au/Al₂O₃ (NaOH) and II: Au/Al₂O₃ (urea). The samples with Al₂O₃ as support were calcined at 523 K.

TABLE 3: Parameters of the Best Fit of the EXAFS Signals of Au References and Au/ Al₂O₃ Samples

sample	coordination number	R [Å]	σ^2 [Å ²]	ΔE [eV]
Au/Al ₂ O ₃ (urea)	8.6 (Au–Au)	2.819	0.0097	7.85
Au/Al ₂ O ₃ (NaOH)	0.4 (Au–O)	2.003	0.0101	6.52
	6.7 (Au–Au)	2.793	0.0101	6.52
Au foil	12 (Au–Au)	2.862	0.0074	9.68

observed, which is a hint for Au–O bonds at this sample. This result agrees with the observations obtained with XPS showing partially oxidic Au at this sample. For an exact quantitative analysis this feature is too small.

EXAFS. Figure 5 shows the modulus of the k^3 weighted Fourier transform of the EXAFS signals (i.e., the pseudo RDF), without phase correction, for both Al₂O₃-supported Au samples in comparison to the gold foil. The Fourier-transformed EXAFS spectrum of the gold foil conforms to the results known from the literature.¹⁹ In the pseudo RDF a significant reduction of the first shell coordination number of both nanoparticle samples is observed, which is more pronounced in the case of NaOH precipitation. The best fits of gold models of the first coordination sphere to the EXAFS signals of the two Al₂O₃-supported samples are presented in Figure 6. Table 3 summarizes the average coordination numbers of the Au to neighbored O and Au atoms, the distance R , the Debye-Waller factor σ and the energy shift ΔE . The obvious difference between the samples is the number of neighboring Au atoms in the first shell, which

is attributed to a smaller average particle size. The XAS measurements therefore confirm the results of the TEM investigations. The reduction of the Au–Au distance in the case of the nanoparticles can be described as a relaxation effect as known from the literature.²⁰ Additionally, a shoulder in the pseudo RDF at about 0.2 nm could be observed for the sample using NaOH as precipitation agent, which seems not to be an artifact. It could be interpreted as an Au–O interaction, as in Au₂O₃ the Au–O distance is about 0.2 nm. Such feature was observed by EXAFS investigations at Au/Al₂O₃ recently published and explained with weak cluster–support interactions.²¹ In this study only metallic gold clusters were detected with XANES; however, the findings of our XANES and XPS measurements indicate some oxidic Au in this sample. The high-resolution TEM images showing in both cases crystalline gold can be explained only by a Au–O interaction located at the particle–support interface or at the surface of the particle because oxygen is too big to occupy octahedral sites in the gold structure without significant distortion.

Discussion

The experimental results clearly show an influence of the precipitation agent on the geometric and electronic structure of the gold particles on alumina as support under the chosen preparation conditions.

The precipitation with NaOH leads to smaller particles with a lower Au–Au coordination number than the preparation with urea. Some hints for a dependence of the particle morphology on the precipitation agents were found, too. Next to these geometric factors a significant difference concerning the Au–O interaction between both samples was observed. For the catalyst prepared with urea, hints for Au–O interactions could not be detected. In contrast, for the sample precipitated with NaOH, the EXAFS investigation gives some hints for O atoms in the neighborhood of the Au atoms. Further evidence for Au atoms interacting with O arises from the XPS and XANES measurements showing partially oxidic Au. According to the results of the high-resolution TEM results, the O atoms seem not to be located inside the gold particles, but at the particle–support interface or adsorbed on the surface of the particles, which cannot be discriminated by our experiments. The observed differences between both samples could be explained by a geometric effect: probably, the Au atoms at the particle–support interface interacting with O atoms of the Al₂O₃ support are oxidized, whereas the atoms inside or at the surface of the particle are zerovalent. The ratio of Au atoms at the particle–support interface to all Au atoms is greater in the case of the smaller and more elongated particles obtained by the preparation

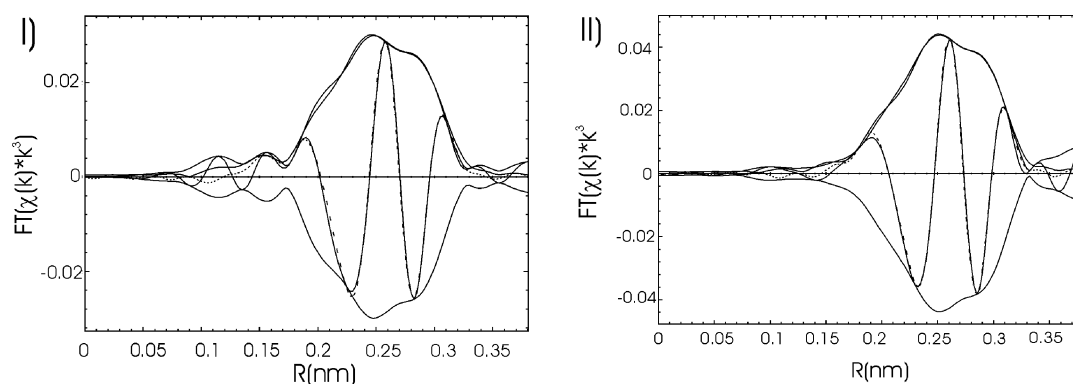


Figure 6. Comparison between the Fourier-transformed EXAFS and the calculated fits as described in the text: I: Au/Al₂O₃ (NaOH); II: Au/Al₂O₃ (urea). The fit parameters are summarized in Table 3.

with NaOH than for the larger and more spherical particles resulting from the precipitation with urea. Thus, the oxidized Au atoms at the interface in the smaller particles could be detected; however, the ratio of Au atoms at the interface would be below the detection limit in the larger particles prepared with urea. Another possible explanation for the differences in the electronic structure are an influence of the precipitation agent on the reducibility of the Au. Such effect was observed for Au/TiO₂, but in contrast to our results, on TiO₂ gold species obtained by preparation with NaOH were reduced more easily than the ones prepared with urea.⁷

The dependence of the particle size and morphology on the precipitation agents suggest different deposition mechanisms for Au depending on the use of NaOH or urea as proposed for Au on TiO₂ formerly.⁷ Analogous to this system, the following mechanisms could be discussed for Au/Al₂O₃: (i) electrostatic interactions lead to the deposition of gold compounds or particles negatively charged on an oxide surface with Al—OH₂⁺ groups, if the pH of the aqueous solution is lower than the isoelectric point of Al₂O₃ (IEP = 8), (ii) the formation of a surface complex by the reaction of the gold hydroxy chlorides and surface OH groups is proposed for the deposition of Au if the pH of the aqueous solution is equal to the IEP of the substrate;²² (iii) with urea the deposition of gold colloids on the oxide surface positively charged followed by the redispersion of these deposited colloids to smaller particles of a few nanometers is discussed. This redispersion is enabled by the increase of the pH from 3 to 7 due to the decomposition of urea. The two latter mechanisms lead to small Au particles of a few nanometers, whereas larger particles are formed by the deposition via electrostatic interaction.²³

The deposition via surface complexes was preferred for the system Au/TiO₂ with NaOH as the precipitation agent with the highest efficiency of gold deposition at pH = 7 which is similar to the IEP of TiO₂. In contrast, our results indicate that the highest amount of deposited gold was reached at pH = 7, which is below the IEP of Al₂O₃. Possible explanations for this behavior could be the amphoteric character of threevalent gold hindering the precipitation of a large amount of gold at pH values higher than 7 or the deposition of a part of the gold via electrostatic interactions between the sites of the oxide surface positively charged and gold compounds with a negatively charged surface. According to results obtained by Wolf and Schüth that the particle size of gold on oxide substrates decreases with increasing pH,²³ which means that a higher amount of OH₂⁺ sites lead to larger particles, the existence of a few gold particles with a diameter above 10 nm could be explained by this gold deposition via electrostatic interactions. Small particles around 2 nm seem to be formed from the gold surface complexes which are products of the interaction between gold hydroxy chlorides and the neutral surface OH sites. Next to this deposition mechanism it is possible that the larger gold particles deposited via electrostatic interactions on the surface disperse to smaller particles, similar to the mechanism discussed for the preparation with urea.⁷ With urea the pH value is increasing during the preparation from 3 to 7 due to the decomposition of the urea, leading to a sequential mechanism: first, at low pH values, the entire gold amount could deposit in the form of large colloids on the surface positively charged; then with increasing pH value, the gold colloids redisperse to small particles. With NaOH the pH value is constant at 7 during the entire preparation. Both processes—deposition and redispersion—occur in parallel, which could explain the smaller particles with a sharper size distribution obtained with NaOH.

The differences between the deposition of gold on TiO₂ published by Zanella et al.⁷ and our results on Al₂O₃ for the preparation with urea could be a consequence of the IEPs, which are different for both oxides. Whereas on TiO₂ with an IEP below 7 no positively charged group exists which allows a complete redispersion of the gold colloids to particles below 2 nm with a sharp size distribution, on Al₂O₃ few positively charged groups remain on the surface. The consequence is that not all deposited gold could redisperse to particles below 2 nm, leading to a larger mean particle size and a broader size distribution than observed for the preparation with NaOH.

These experimental results obtained by spectroscopy and microscopy allow us to explain the different chemical activities of the Al₂O₃-supported gold nanoparticles depending on the precipitation agent in the partial oxidation of polyvalent oxygen-substituted compounds.⁸ The higher activity of Au catalysts prepared with NaOH could be a consequence of the smaller particle size observed by TEM and the lower Au—Au coordination number found by the EXAFS measurements compared to the sample with urea as precipitation agent. Especially, the availability of low coordinated sites was proposed to be crucial for the activity of Au particles.²⁴ The high activity of low coordinated Au atoms to dissociate oxygen could facilitate the oxidation at these smaller particles. A positive influence of oxidic Au observed at the samples prepared with NaOH on the activity cannot be excluded from our investigation.

Conclusions

An influence of the precipitation agent on Au—Au coordination number, size, and probably morphology of the gold particles deposited on Al₂O₃ was observed. Whereas with NaOH as precipitation agent a Au—Au coordination number of 6.7 and a mean particle size below 2 nm with a rather sharp distribution could be found, precipitation with urea leads to a coordination number of 8.6 and a mean particle size around 3 nm with a significant broader distribution. From TEM results a rather lenticular morphology of the particles of the sample prepared with NaOH could be concluded. At this sample, O was found in the neighborhood of some Au atoms, leading to partially oxidic Au. All these experimental findings support the thesis of two different deposition mechanisms depending on the precipitation agent. Further investigations of these mechanisms require appropriate in situ measurements.

Acknowledgment. The authors thank I. Pitsch for catalyst preparation and discussion and G. Klinger for technical assistance. We are grateful to HASYLAB for the provision of beamtime at the experimental station A1. This work was supported by the Federal Ministry of Education and Research of Germany (project 03C3013), the EU (European Fund for Regional Development), and the Senate Department of Science, Research and Culture of Berlin.

References and Notes

- (1) Haruta, M.; Yamada, N.; Kobayashi, T.; Iijima, S. *J. Catal.* **1989**, *115*, 301.
- (2) Haruta, M. *Catal. Today* **1997**, *36*, 153.
- (3) Bond, G. C.; Thompson, D. T. *Catal. Rev.—Sci. Eng.* **1999**, *41*, 319.
- (4) Haruta, M. *Chem. Record* **2003**, *3*, 75.
- (5) Tsubota, S.; Cunningham, D. A. H.; Bando, Y.; Haruta, M. *Stud. Surf. Sci. Catal.* **1995**, *91*, 227.
- (6) Zanella, R.; Giorgio, S.; Henry, C. R.; Louis, C. *J. Phys. Chem. B* **2002**, *106*, 7634.
- (7) Zanella, R.; Giorgio, S.; Shin, C.-H.; Henry, C. R.; Louis, C. *J. Catal.* **2004**, *222*, 357.

- (8) Berndt, H.; Martin, A.; Pitsch, I.; Prütse, U.; Vorlop, K.-D. *Catal. Today* **2004**, *91*–92, 191.
- (9) Lopez, N.; Janssens, T. V. W.; Clausen, B. S.; Xu, Y.; Mavrikakis, M.; Bligaard, T.; Nørskov, J. K. *J. Catal.* **2004**, *223*, 232.
- (10) Valden, M.; Lai, X.; Goodman, D. W. *Science* **1998**, *281*, 166.
- (11) Mimicò, S.; Scirè, S.; Crisafulli, C.; Visco, A. M.; Galvagno, S. *Catal. Lett.* **1997**, *47*, 273.
- (12) Guillemot, D.; Borovkov, V. Yu.; Kazansky, V. R.; Polisset-Thfoin, M.; Fraissard, J. J. *Chem. Soc., Faraday Trans.* **1997**, *93*, 3587.
- (13) Rageyama, H.; Tsubota, S.; Kadono, K.; Fukumi, K.; Akai, T.; Haruta, M. *J. Phys. IV* **1997**, *7*, C2–935.
- (14) Bocuzi, F.; Chiorino, A.; Manzoli, M.; Andreeva, D.; Tabakova, T. *J. Catal.* **1999**, *188*, 176.
- (15) Berndt, H.; Pitsch, I.; Evert, S.; Struve, K.; Pohl, M.-M.; Radnik, J.; Martin, A. *Appl. Catal., A* **2003**, *244*, 169.
- (16) Ressler, T. *J. Synchrotron Radiat.* **1998**, *5*, 118.
- (17) Zabinsky, S. I.; Rehr, J. J.; Ankudinov, A.; Albers, R. C.; Eller, M.-J. *Phys. Rev. B* **1995**, *52*, 2995.
- (18) Dalacu, D.; Klemberg-Sapieha, J. E.; Martinu, L. *Surf. Sci.* **2001**, *472*, 33.
- (19) Weiher, N.; Willneff, E. A.; Figulla-Kroschel, C.; Jansen, M.; Schroeder, S. L. M. *Solid State Commun.* **2003**, *125*, 317.
- (20) Balerna, A.; Bernieri, E.; Picozzi, P.; Reale, A.; Santucci, S.; Burattini, E.; Mobilio, A. *Surf. Sci.* **1985**, *156*, 206.
- (21) Weiher, N.; Bus, E.; Delannoy, L.; Louis, C.; Ramaker, D. E.; Miller, J. T.; van Bokhoven, J. A. *J. Catal.* **2006**, *240*, 100.
- (22) Machesky, M. L.; Andrade, W. O.; Rose, A. W. *Geochim. Cosmochim. Acta* **1991**, *5*, 769.
- (23) Wolf, A.; Schüth, F. *J. Appl. Catal., A* **2002**, *226*, 1.
- (24) Lopez, N.; Nørskov, J. K. *J. Am. Chem. Soc.* **2002**, *124*, 11262.